

The unresolved mystery of dust particle swarms within the magnetosphere

Max Sommer^{1,2}

¹University of Stuttgart, Germany

²University of Cambridge, UK

13 May 2024

Abstract

Early-generation in-situ dust detectors in near-Earth space have reported the occurrence of clusters of sub-micron dust particles that seemed unrelated to human spaceflight activities. In particular, data from the impact ionization detector onboard the HEOS-2 satellite indicate that such swarms of particles occur throughout the Earth's magnetosphere up to altitudes of 60 000 km—far beyond regions typically used by spacecraft. Further account of high-altitude clusters has since been given by the GEO-deployed GORID detector, however, explanations for the latter have so far only been sought in GEO spaceflight activity.

This perspective piece reviews dust cluster detections in near-Earth space, emphasizing the natural swarm creation mechanism conjectured to explain the HEOS-2 data—that is, the electrostatic disruption of meteoroids. Highlighting this mechanism offers a novel viewpoint on more recent near-Earth dust measurements. We further show that the impact clusters observed by both HEOS-2 and GORID are correlated with increased geomagnetic activity. This consistent correlation supports the notion that both sets of observations stem from the same underlying phenomenon and aligns with the hypothesis of the electrostatic breakup origin. We conclude that the nature of these peculiar swarms remains highly uncertain, advocating for their concerted investigation by forthcoming dust science endeavours, such as the JAXA/DLR DESTINY+ mission.

1 Introduction

Since the first reliable and highly sensitive in-situ dust detectors were deployed in the 1970s, the clustering of dust particles, that is, the occurrence of multiple impacts on timescales of minutes or hours, has been a commonly observed phenomenon in near-Earth space. In particular, it was the impact ionization detectors onboard the satellites Prospero and HEOS-2 that gave the first conclusive account of such clusters (Bedford and Sayers, 1973; Hoffmann et al., 1975a). This detector type registers the plasma generated in hypervelocity impacts of micron and sub-micron particles, and posed a major improvement over previous designs, such as the microphone-type sensors, which proved to be highly susceptible to the detection of spurious events (McDonnell, 1978). The detected clusters were interpreted as spatially confined swarms of micrometeoroids, encountered by the spacecraft. Such formations of particles would be expected to rapidly disperse, and thus, an active mechanism that continuously created these clusters would be required. This led Fechtig and Hemenway (1976) to propose that the clusters are generated by the fragmentation of larger meteoroids, for instance, through phase-change-induced or electrostatically-driven disruption triggered upon entering the ionosphere. Analysing the HEOS-2 dust counter data, which covered a broad range of distances from Earth due to the satellites highly elliptic orbit, Fechtig et al. (1979) (in the following referred to as F79) conclude that rather confined particle swarms, presumably generated by the electrostatic breakup of fluffy meteoroids, occur throughout the Earth's magnetosphere, that is, up to altitudes of roughly 60 000 km. Further account of clustering was given by several other dust counter instruments, in particular in low Earth orbit (LEO), such as those onboard the Long Duration Exposure Facility (LDEF, launched 1984) and other satellites (see Section 2.1), as well as at altitudes beyond LEO by the Munich Dust Counter (MDC, 1990) and the Geostationary Orbit Impact Detector (GORID, 1996).

Some clusters detections during these later missions could be attributed to human spaceflight activities, in particular, to specific firings of solid rocket motors (SRMs) (e.g., Schobert and Paul, 1997). SRMs produce large amounts of solid combustion products in the form of micron-sized aluminium oxide particles, which, if used for geostationary orbit (GEO) insertions or retrograde LEO deorbiting manoeuvres, can create circumterrestrial streams of micro-debris with lifetimes of up to months (Bunte, 2003; Stabroth et al., 2008). As the use of orbital SRMs ramped up in the late 1970s and 1980s (to

enable utilization of the GEO, see e.g., [McDowel, 1997](#); [Wegener et al., 2004](#)), they gained attention for their potential to cause hazard to spacecraft through their generated micro-debris trails ([Mueller and Kessler, 1985](#); [Akiba and Inatani, 1990](#))—amidst the growing awareness of the space debris problem in general ([Kessler and Su, 1985](#); [Kessler, 1991](#)). In fact, the analysis of impacts on retrieved spacecraft surfaces showed that, in LEO, the debris dust flux dominates over the natural dust flux ([Laurance and Brownlee, 1986](#); [Graham et al., 2001](#); [Hörz et al., 2002](#)).

Following this increased scrutiny of dust sources from human activity, clustered impacts recorded by the GEO-deployed GORID were generally attributed to micro-debris ([Drolshagen et al., 2001a,b](#)), even though only few such events could be directly linked to SRM firings. It appears that earlier hypotheses regarding natural particle swarms occurring throughout the magnetosphere, as indicated by HEOS-2 data—remarkably, recorded prior to the extensive utilization of the GEO—were not considered in the analysis of the GORID data. However, aspects of HEOS-2 and GORID-detected clusters suggest that both studies may have observed the same phenomenon. In this perspective, we first review the measurements of particle clusters in near-Earth space in general in Section 2. In Section 3, we then reassess the observations of HEOS-2 and GORID of clusters observed beyond LEO (i.e., those by HEOS-2 and GORID), under the premise that both instruments have observed the ‘magnetospheric swarms’ postulated by [F79](#). We also provide an outlook for the future investigation of this phenomenon by the upcoming DESTINY+ mission.

2 Measurements and interpretations of near-Earth dust clusters

2.1 At LEO altitudes

The multitude of dust-counter-type instruments deployed in LEO gathered extensive evidence for clustered impacts of submicron and micron-sized particles at such altitudes. The first such account was given by the impact ionization detector onboard the Prospero satellite, which registered large variations in the daily impact rate, suggesting that around 64% of impacts occurred in clusters ([Bedford et al., 1975a,b](#)). In search for explanations, there was cautious speculation that meteoroids grazing the Earth’s atmosphere could break up and shed a swarm of sub-micron fragments, which would then be intercepted by the spacecraft ([Bedford et al., 1975a](#)). (This mechanism was later ruled out for swarms observed at higher altitudes, see Section 2.2.1.) Similarly, the capacitor-type dust detector onboard Explorer 46 reported variations in the daily impact rate, which were attributed to the presence of submicron particles within known meteor showers ([Singer and Stanley, 1980](#))—contrary to the theoretical expectation of micro-particle-depleted streams due to the action of radiation pressure (e.g., [Dohnanyi, 1972](#)).

Conclusive evidence for the occurrence for compact particle clusters in LEO was eventually given by the high-time-resolution dust counters onboard LDEF, which occasionally recorded bursts of impacts with instantaneous rates up to four orders of magnitude higher than the mean rate ([Oliver et al., 1995](#)). Some of these bursts were seen repeatedly at certain points along the spacecraft orbit, indicating intersections with distinct circumterrestrial dust streams, thus interpreted to stem from human activity ([Cooke et al., 1995](#)). Two of those repeating clustering events could then indeed be linked to the exhaust dust streams of specific SRM firings ([Schobert and Paul, 1997](#); [Stabroth et al., 2007](#)). However, the origin of most of the detected clusters remained unresolved.

Further confirmation that the majority of dust impacts in LEO occurs in clusters, some of which representing circumterrestrial streams, has since been given by the dust-counter-type instruments SPADUS ([Tuzzolino et al., 2005](#)), DEBIE-1 & 2 ([Schwanethal et al., 2005](#); [Menicucci et al., 2013](#)), and SODAD-1 & 2 ([Durin and Mandeville, 2009](#); [Durin et al., 2016, 2022](#)). One of the streams detected by SPADUS could be attributed to a known SRM firing ([Neish et al., 2004](#); [Bunte and Drolshagen, 2005](#)), whereas another one appeared to be associated with the explosion of a launch vehicle upper stage ([Tuzzolino et al., 2001](#)).

2.2 Beyond LEO

While the occurrence of clusters in the densely-populated LEO region may plausibly be the result of human activity in a number of ways (i.e., collisions and explosions of satellites or debris, orbital SRM firings, substances released by crewed spacecraft, etc.), the occurrence of clusters at higher altitudes is more difficult to explain. Nonetheless, evidence for their existence has been gathered by a few in-situ dust detectors, which are reviewed in the following.

2.2.1 HEOS-2

The first and most extensive account of particle clusters at altitudes beyond LEO was given by the dust counter onboard HEOS-2. The HEOS-2 spacecraft, launched in 1972, carried an impact ionization detector on a highly eccentric orbit with

varying perigee in a range of 350–3000 km and apogee of 240 000 km, as illustrated in Figure 1. Due to that orbit, HEOS-2 could sample the dust flux over a wide range of altitudes, from an almost ‘pristine’ interplanetary background flux around its apogee, all the way to the near-Earth dust flux at only a few 1000 km altitude. Besides an interplanetary sporadic flux described by random impacts, the HEOS-2 data indicated the presence of two types of cluster phenomena: (1) the ‘swarms’, which were characterized by short intervals between consecutive impacts of up to 15 minutes, and (2) the ‘groups’, with longer intervals of up to 12 hours (Hoffmann et al., 1975a,b; Fechtig et al., 1979).

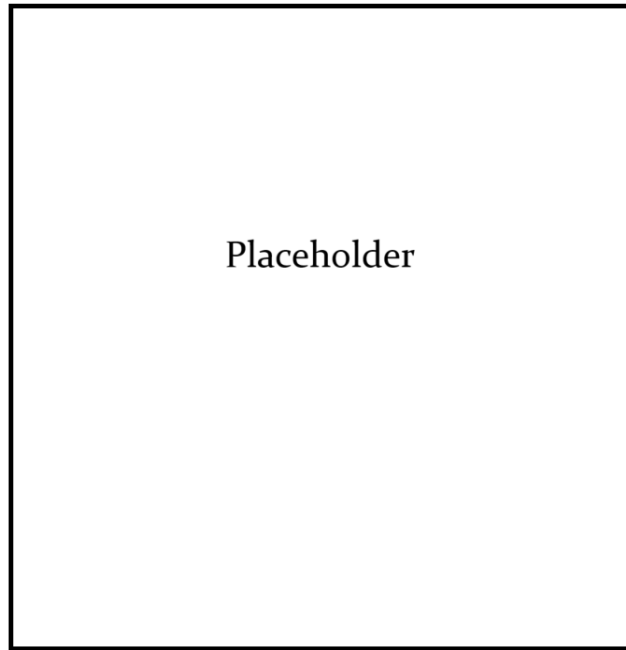


Figure 1: Illustration of the HEOS-2 orbit through the plasma and field regions of the Earth’s magnetosphere. Reproduced from Fechtig et al. (1979). (Due to copyright restrictions this figure is only included in the journal version of this article.)¹

The swarms were exclusively encountered at distances of up to 10 Earth radii (R_{\oplus}), which is about the extent of the Earth’s magnetosphere dipole field (about twice the GEO altitude). These ‘magnetospheric swarms’ generated an averaged particle flux rate about one order of magnitude above the sporadic background. Examining different sensor viewing directions perpendicular to the Sun—namely, the Earth apex, antapex, ecliptic north, and south—HEOS-2 also revealed that the swarms occurred anisotropically, with a slight preference for the Earth apex direction (F79). The derived masses of the individual particles ranged mostly within 10^{-14} g to 10^{-12} g,² similar to the largest of the hyperbolic β -meteoroids irradiating from the Sun (e.g., Wehry and Mann, 1999), which however the HEOS-2 sensor was insensitive to, due to its pointing. Impact speeds of the swarm particles derived by rise time analysis of the impact charge signal were found to be in the order of $4\text{--}16\text{ km s}^{-1}$.

F79 show that the swarms could be caused by the breakup of fluffy interplanetary meteoroids that fragment due to inner, repulsive electrostatic forces (a mechanism first described by Öpik, 1956), resulting from being charged up to high potentials while traversing the Earth’s magnetosphere. From the number of registered impacts and the total encounter duration of each detected swarm, they estimate the total numbers of particles per swarm to fall in the range from 10^{14} to 10^{19} , corresponding to individual parent meteoroid masses between 10 g and 1000 kg (F79), with a geometric mean of 5.2 kg. (Note that the largest observed swarm, corresponding to a progenitor of nearly 1000 kg, appears to be divided into four sub-swarms, suggesting the breakup of multiple smaller objects in close temporal proximity.) Such meteoroids should be observable as visible bright meteors, also called ‘fireballs’, when entering the atmosphere. The meteoroids producing the Ceplecha type III fireballs, which show high ablation ability and are thus thought to stem from low-bulk-density meteoroids (Ceplecha, 1977; Ceplecha et al., 1998), are considered by F79 the most likely candidates for the swarm progenitors. These low-density-type meteors, however, are associated with cometary source orbits that generally produce high atmospheric entry velocities ($20\text{--}70\text{ km s}^{-1}$), which is incompatible with the rather low-velocity swarms. F79 acknowledge a lack of low-velocity type III fireballs, which

¹Journal version of this article: <https://doi.org/10.1098/rsta.2023.0370>

²Corresponding to particle radii of about 100–500 nm, or β factors of in the order of 0.5–1.

could represent the sought-after swarm progenitors, but note that this apparent deficiency could potentially be explained by selection effects in meteor observations as well as swarm production. Based on the swarms' directionality, they rule out creation via aero-fragmentation (the speculated origin of the Prospero clusters, see Section 2.1) or a relation to meteor showers (Dohnanyi and Fechtig, 1977; Fechtig et al., 1979).

The more spread-out 'groups', on the other hand, were detected at all distances from Earth (i.e., up to the satellite's apogee of around 240 000 km), yet crucially, they appeared almost exclusively when the Moon was within the sensor's field of view (Hoffmann et al., 1975a; Fechtig et al., 1979). Backtracing of the group particles' trajectories further substantiated the idea of a lunar origin (Hoffmann et al., 1975b). Consequently, the authors interpreted these groups as originating from occasional larger meteoroid impacts on the Moon that would create significant amounts of ejecta escaping lunar gravity, subsequently roaming through the Earth-Moon system in somewhat dispersed formations of particles. By modelling the motion of escaping ejecta clouds through the Earth-Moon system, it was further concluded that their expected spatial dimensions are consistent with HEOS-2's encounter times of the groups, and that lunar impactors in the order of 1 kg could suffice to create the observed group number densities (Dohnanyi, 1977). Attempts to correlate the occurrence of groups with lunar impact events sensed by Apollo-deployed seismometers were inconclusive, due to the much higher number of seismic events compared to group detections (F79). In this paper, we will not consider these lunar-origin clusters further, and instead focus on the near-Earth swarms observed by HEOS-2.

2.3 Munich Dust Counter

The findings of HEOS-2 are reinforced by the data of the impact-ionization-type Munich Dust Counter (MDC) onboard Hiten, launched in 1990. As HEOS-2, the Hiten spacecraft was placed on a highly eccentric orbit with initial perigee of a few 1000 km and apogee of 300 000 km. MDC, similarly to the HEOS-2 detector, reported a ten-fold increase of flux in regions near Earth (closer than 100 000 km) compared to interplanetary space and an anisotropy in the flow direction, with a preference for the Earth apex direction (Iglseider et al., 1993a,b). In addition, strong clustering with instantaneous particle rates of up to five orders of magnitudes over the mean flux was observed. Unfortunately, however, no further details about the MDC-detected clusters have been published.

2.4 GORID

The Geostationary Orbit Impact Detector (GORID) was a refurbished engineering model unit essentially identical to the impact ionization dust detectors flown on the interplanetary probes Ulysses and Galileo (Grün et al., 1992a,b). GORID was mounted on the Russian telecom satellite Express-2, which was placed in GEO in 1996 (Drolshagen et al., 1999). GORID data indicated a significant excess of clustered impacts, which were characterized by separations in time from minutes to an hour, dominating over random impacts by a factor of about four (Drolshagen et al., 2001a; Graps et al., 2007). Similarly to the case of LDEF, few clusters were observed recurrently at certain points along the orbit, and could be dynamically linked to the exhaust dust streams of specific SRM firings (Bunte, 2003; Bunte and Drolshagen, 2005). The vast majority of detected clusters, however, were non-recurrent and could not be attributed to any specific source. This led Bunte and Drolshagen (2005) to conjecture an unknown micro-debris-cloud-generating mechanism present at GEO altitudes. In that sense, it was speculated that the breakup of larger SRM slag particles via electrostatic fragmentation could act as such a mechanism (Graps et al., 2007).³

Ultimately, all GORID-detected clusters were attributed to debris-related phenomena (Drolshagen et al., 2001a; Graps et al., 2007) with no consideration of the possibility that the clusters are of natural origin. One reason for this is that the impact velocities inferred from charge signal rise times indicate most impactors to have slow speeds ($<5 \text{ km s}^{-1}$), which would be compatible with relative speeds of debris in GTO-like orbits. However, it is noted that these impact speeds had been found to be unreliable for a number of reasons. In particular, impacts on the insides of the detector's side walls instead on the impact target would generate events with abnormally long rise times, and thus appear as slow, even though they are not (see also Stübig, 2002; Altobelli et al., 2004; Willis et al., 2004, 2005). Later analysis of the GORID data therefore ignores the rise-time-derived speeds altogether (Graps et al., 2007). By geometrical consideration, one might expect that around half of the impacts inside the detector occur on the side walls (assuming an isotropic flow).⁴

³SRM slag particles are larger (up to cm-sized) aluminium-oxide clumps ejected at the end of an SRM burn with low relative velocity (Jackson et al., 1997). Fragments of slag produced in GEO insertions (consequently exhibiting near-GEO orbital parameters) would have too-low velocities relative to GORID (few 100 m s^{-1}) to be efficiently detected via impact ionization. However, GTO insertions would produce slag with velocities relative to GORID of $1.5\text{--}2 \text{ km s}^{-1}$.

⁴The effective solid angle Ω_{eff} of GORID including its inner side walls can be approximated by an unobstructed plate detector with the same nominal

One striking feature of the GORID-observed clusters is the strong modulation of their occurrence with the local time of the satellite. Clusters were detected with a strong preference around local midnight, that is, when the satellite was on the Sun-opposing side of the Earth, and the spacecraft-body-fixed sensor was sensitive to a flux from the Earth apex direction (Bunte and Drolshagen, 2005; Graps et al., 2007). For the half of the orbit, when the sensor was pointing away from apex, virtually no clusters were detected. There is no obvious reason why debris would preferentially be located around local midnight, although Graps et al. (2007) note that an unknown process occurring only in the magnetotail region might facilitate debris cluster detections.

Another noteworthy feature is that the distribution of the impact-generated ion grid charges (Q_i) shows a greater tendency towards smaller charges for clustered impacts compared to random events (Graps et al., 2007). This trend could imply a steeper mass distribution, possibly indicating an increased prevalence of smaller particles within clusters.

Lastly, measurements of GORID’s charge-sensitive entry grids indicated that cluster particles were highly negatively charged (Bunte et al., 2006; Graps et al., 2007), as opposed to the positive equilibrium potential particles are thought to assume in interplanetary space as well as inside the magnetosphere under average conditions (Horányi, 1996). Positive charges, however, occurred only among the randomly impacting particles, according to the GORID measurements.

3 Discussion

3.1 HEOS-2 and GORID clusters - a common origin?

Having reiterated the main findings about dust particle clusters in near-Earth space, we will now reassess them in context to each other. In particular, we will attempt to reconcile the high-altitude clusters observed by HEOS-2 and GORID, which have garnered notably different interpretations. The fact that both instruments reported an apparent anisotropy favouring the Earth apex, and typical cluster encounter durations of up to 90 minutes suggests that they are related to each other, and thus, that they could stem from the same phenomenon. In the following, we will discuss several aspects that could support this notion—specifically, F79’s hypothesis of the magnetospheric swarms—and weigh in on potential swarm progenitor candidates, as well as other explanations for the observed clusters.

3.1.1 Anisotropy

Both instruments reported preferential detection of clusters when exposed to the Earth apex direction, although the observed anisotropy was arguably more pronounced for GORID than for HEOS-2 (compare, e.g., F79 Tab. 7 with Graps et al. (2007) Fig. 2). Interestingly, although the GORID data indicate a strong preference for cluster detection when exposed to the Earth apex, the effective sensitivity towards that direction remained relatively low. Due to GORID’s body-fixed mounting on the GEO satellite with a boresight pointing only 25° away from equatorial north, the minimum angle between boresight and the apex direction (which was achieved once per day, during local midnight on the geostationary orbit) varied between 42° and 88° , depending on the time of the year. Thus, considering GORID’s angular sensitivity profile (Grün et al., 1992a), one would expect a distinct seasonal modulation of cluster detections, if the clusters were indeed coming preferentially from the apex direction. The maximum cluster occurrence rate should occur in autumn when the sensor’s exposure to the Earth apex direction is highest (during local midnight hours), whereas the minimum rate should occur in spring. To check this proposition, the mean flux of clustered events during each calendar month averaged over the mission duration is shown in Figure 2, alongside the minimum angle between sensor boresight and the apex direction. Although the highest rates are indeed observed in autumn, the minimum detection rate of clusters occurs in summer. Thus, a clear correlation of the cluster occurrence rate with the sensor’s sensitivity toward the Earth apex direction is not evident.

A reduced modulation of rates with the exposure to the apex could be due to the sensor’s asserted sensitivity to wall impacts (Stübig, 2002; Altobelli et al., 2004), which considerably widens the angular sensitivity profile. On the other hand, the lack of a clear modulation throughout the year in combination with the observed strong modulation with local hour, indicates that it is not the sensor’s exposure to the apex direction that is the crucial factor for cluster detection, but rather the location of the spacecraft on the tail side of the magnetosphere. The tail side could indeed be preferential for the detection of the putative magnetospheric swarms, due to the proximity to the magnetosphere’s plasmashet. The plasmashet, with its elevated electron fluxes, had been suggested by F79 as another potential swarm genesis region, besides the field line regime connected to the auroral zones traversed by HEOS-2 (F79).

sensitive area (all particles entering the instrument are detected), which has $\Omega_{\text{eff}} = \pi$ sr. The Ω_{eff} of the GORID impact target is 1.45 sr (Grün et al., 1992a). Thus, the Ω_{eff} of just the inner walls (1.69 sr, calculated as the remainder of the two) is comparable to that of the impact target.

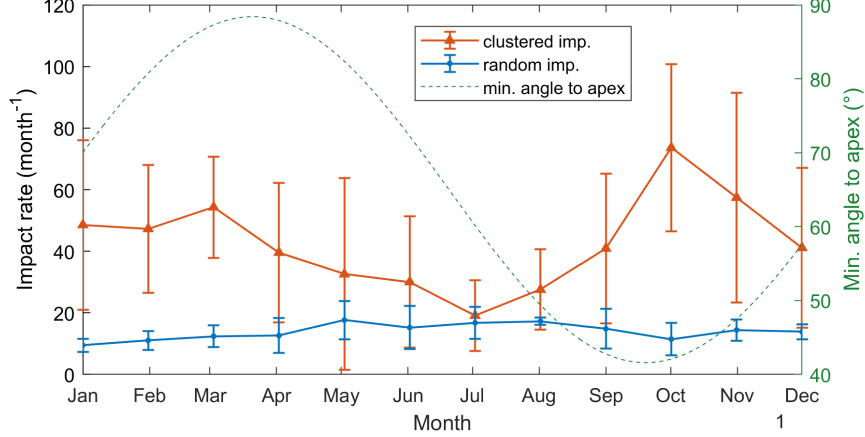


Figure 2: Monthly mean impact rates recorded by GORID per calendar month averaged over the entire observing period (1997–2002). Error bars represent the year-to-year standard deviation. Based on data from Drolshagen (2006). Also shown is the minimum angle between the sensor boresight and the Earth apex direction (reached once per day at local midnight) over the course of the year.

3.1.2 Geomagnetic activity

Considering that F79 identified high fluxes of energetic electrons (>10 keV) in the surrounding plasma as a crucial factor for charging up meteoroids enough to cause their electrostatic breakup (F79), it is reasonable to assume that the occurrence of swarms is correlated with geomagnetic activity. Plasma motion and electric currents inside the magnetosphere are enhanced during geomagnetic storms, which are driven by solar wind disturbances, which in turn are produced by solar activity (Richardson et al., 2000). We may thus analyse the occurrence of clusters registered by HEOS-2 and GORID in the context of the solar cycle timing and the geomagnetic activity level.

The observation period of HEOS-2 (1972–1974) occurred well after the peak of solar cycle 20 (1969), and during the cycle’s decline (minimum in 1976). A cycle’s declining phase is typically not associated with major geomagnetic storms, due to the less frequent occurrence of coronal mass ejections (CMEs). The decline of solar cycle 20, however, was marked by a period of exceptionally high geomagnetic activity occurring in 1973–1975, caused by persistent high-speed solar wind streams (Gosling et al., 1977; Richardson et al., 2000; Richardson and Cane, 2012). High fluxes of energetic electrons, in particular, are associated with high-speed streams (Reeves et al., 2011; Boynton et al., 2013). Notably, HEOS-2 detected 13 of the 15 swarms in 1973 and 1974, even though this period corresponded to only 64% of the observation time. To test whether the occurrence of particle swarm events correlates with elevated geomagnetic activity, we can analyse the ‘ Kp index’ preceding these events. The Kp index, derived from geomagnetic observatory data at a 3-hour interval, provides a standardized measure of global geomagnetic activity levels on a scale from 0 to 9, with higher values indicating increased disturbance, and has been recorded for more than 70 years (Matzka et al., 2021b). Our analysis shows that, compared to the overall mean Kp index of 2.45 (SD = 1.38) over the mission duration, the mean of the Kp indices directly preceding a HEOS-2 swarm detection is notably higher at 3.46 (SD = 1.19). This difference is statistically significant, as supported by the obtained p -value of 0.005 from a two-sample t -test, suggesting that there is only a 0.5% probability of observing such a difference in means if there was no correlation. These findings indicate a preferential association between particle swarm detections and heightened geomagnetic activity, as reflected by the Kp index. This is also illustrated in Figure 3 (top), which shows the timings of HEOS-2 swarm detections next to the Kp index (averaged for 5-day intervals).

The observation period of GORID (1997–2002) covers the rising phase and maximum of solar cycle 23 (min. in 1996 and max. in 2001). In the case of GORID, our dataset is limited to the monthly mean detection rate of clustered impacts (Drolshagen, 2006), rather than the precise timings of cluster detections. Therefore, we compare the cluster impact rate also to the monthly mean Kp index, as depicted in Figure 3 (bottom). This comparison reveals a correlation between the cluster detection rate and the geomagnetic activity level, quantified by the Pearson correlation coefficient r . While for the random event rate we obtain $r = -0.11$ (indicating no correlation), the cluster rate shows a moderate correlation with $r = 0.57$.

It is important to note that the electron fluxes might not always be directly correlated with the Kp index. In particular, the pumping of fluxes of relativistic electrons (>1 MeV) by geomagnetic storms is known to be time-delayed and can cause elevated levels lasting for several days after a storm has subsided (Baker et al., 1998; Friedel et al., 2002; Boynton et al.,

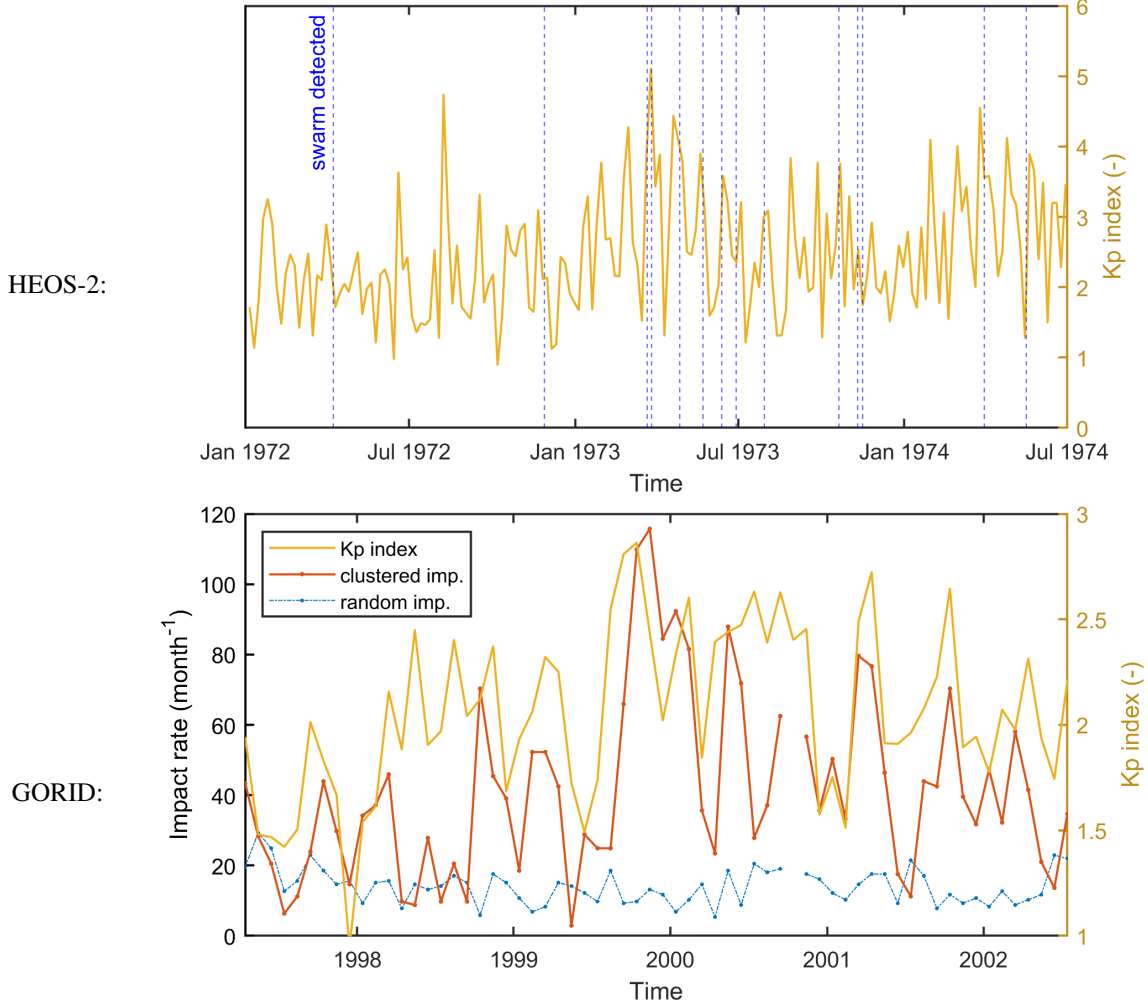


Figure 3: Cluster occurrence with respect to geomagnetic activity. (Top) Times of swarm detections by HEOS-2 over the entire observing period (obtained from F79), indicated by vertical blue lines. Also shown is the average Kp index for 5-day intervals, indicating the level of geomagnetic activity. (Bottom) Monthly mean detection rates recorded by GORID of random and clustered impacts over the entire observing period (obtained from Drolshagen (2006), considering only ‘class 3’ events, supposed to be real impacts). Also shown is the average Kp index for each month. Kp index data for both plots was obtained from Matzka et al. (2021a,b).

2013). Conditions facilitating swarm formation may thus persist beyond geomagnetic activity peaks. Nevertheless, the fact that both HEOS-2 and GORID detected clusters preferentially during periods of high geomagnetic activity further hints at a common phenomenology.

The notion that swarm creation is associated with high geomagnetic activity is also consistent with the findings of Graps and Grün (2000), who modelled the equilibrium potentials of grains within the magnetosphere for ‘quiet’ and ‘active’ conditions, as well as for different particle materials. They conclude that, while quiet conditions usually generate positive potentials (<15 V), disturbed conditions can produce highly negative potentials (<-1000 V) for materials with low photoelectron yield.

3.1.3 Impact rates

We may also compare the incidence rates of clustered impacts between HEOS-2 and GORID. Table 1 summarizes the key geometrical characteristics of both sensors, the nominal sensitive area A_0 , the maximum entry angle θ_{\max} , the effective solid angle Ω_{eff} , and the geometric factor G , which is the product of A_0 and Ω_{eff} , and represents the effective gathering power of an instrument with respect to an isotropic flux. These parameters allow us to relate the impact rates onto HEOS-2 and GORID

to one another. For a collimated dust stream and a directly upstream-pointing sensor, only the nominal sensitive area A_0 is relevant, such that GORID would be exposed to about 10 times as many impacts as the HEOS-2 detector. For an isotropic flow of dust (or a randomly varying instrument pointing) the geometric factor G is the relevant characteristic, such that GORID would be exposed to about 15 times as many impacts as HEOS-2.

Table 1: Comparison of sensor geometries.

Instrument	A_0 cm ²	θ_{\max} °	Ω_{eff} sr	G cm ² sr
GORID (Grün et al., 1992a)	1000	70	1.45	1450
GORID incl. walls (approx.)	1000	90	3.14	3140
DDA (Sommer, 2024)	300	45	0.48	144
HEOS-2 (Hoffmann et al., 1975b)	95.4	60	1.03	98

With HEOS-2, a total of 207 swarm particles (split among 15 swarms) have been identified during an accumulated observation time below $10 R_{\oplus}$ of 70 days (F79). This amounts to an average incidence rate of 2.9 day^{-1} . On the other hand, GORID detected a total of 2477 clustered events during a total observation time of 1827 days (Drolshagen, 2006; Graps et al., 2007), amounting to a mean rate of 1.4 day^{-1} . (This only represents ‘class 3’ events, i.e., those with the highest confidence of being real impacts.) Since the GORID sensor has a gathering power of about 15 times that of HEOS-2, it effectively detected a 30 times lower flux of clustered impacts than HEOS-2.⁵ If the clusters detected by HEOS-2 and GORID stem for the most part from the same phenomenon (presumably, the magnetospheric swarms), the discrepancy may be explained by the following reasons:

- The HEOS-2 sensor was more exposed to the anisotropic flow of swarms than GORID, which both instruments indicated to be coming preferentially from the Earth apex: HEOS-2 pointed straight towards the Earth apex for 40% of the observation time. GORID, on the other hand, was only marginally exposed to the apex direction, as discussed in Section 3.1.1.
- The HEOS-2 sensor was more sensitive than GORID, and thus could detect more particles. The particle mass detection threshold of the HEOS-2 detector is indeed reported to be one order of magnitude lower than that of GORID at the same velocity: $m_{\min, \text{HEOS}} = 1.2 \times 10^{-15} \text{ g}$ and $m_{\min, \text{GORID}} = 1.5 \times 10^{-14} \text{ g}$, both at $v_{\text{imp}} = 10 \text{ km s}^{-1}$ (Dietzel et al., 1973; Göller and Grün, 1989). Particle masses derived from HEOS-2 measurements indicate that swarm particles are partially below the GORID threshold (F79).
- More swarms occurred at the location of the HEOS-2 satellite, which flew through the pole regions of the magnetosphere, as opposed to GORID, which orbited in the equatorial plane. Or, more swarms occurred during the time of the HEOS-2 mission, potentially as a result of varying geomagnetic activity (see Section 3.1.2).

Given the above considerations, the rates as of GORID and HEOS-2 are arguably reconcilable, which upholds the notion that the clusters detected by both instruments could stem from the same phenomenon.

3.1.4 Swarm progenitor candidates

We have already mentioned the apparent deficiency of low-velocity, low-bulk-density meteors, whose progenitors could be the source of the swarms, yet which might not have been observed due to selection effects, as noted by F79. Especially considering the large masses derived by F79 for these progenitors of 10 g to 1000 kg (geom. mean of 5.2 kg), the lack of their detection as meteors poses a conundrum. In addition, Mendis (1981, 1984) showed that—while conceivable for smaller grains—such large meteoroids would have to exhibit improbably small tensile strengths in order to electrostatically disrupt. Rather than complete disruption, they suggest that irregularly shaped meteoroids would be electrostatically ‘eroded’, as edges and protrusions are more readily chipped by the electrostatic tension (Hill and Mendis, 1981), thereby shedding the material to generate the swarms. As only a fraction of the bulk mass could be shed by this erosion, however, even larger meteoroids would be required to yield the swarm masses estimated by F79.

⁵This discrepancy increases by a factor of ~ 2 if wall impacts are considered for GORID, due to a doubling of its geometrical factor. The discrepancy decreases by 33% if wall impacts are considered for both instruments.

Similarly speculative, one might consider the possibility that it is not the disruption of a single massive progenitor that produces the swarms, but rather the quasi-simultaneous electrostatic breakup of numerous micrometeoroids within a certain volume of space. Given the asserted correlation of swarm detection with geomagnetic activity (see Section 3.1.2), it is conceivable that local intensity spikes of the plasma environment could cause the disruption of micron- and millimetre-sized particles within a whole region of the magnetosphere (for a review of turbulences of the magnetosphere, see, e.g., [Zimbardo et al., 2010](#)). Although only two of the 15 swarms detected by HEOS-2 exhibited a clear substructure (hinting at multiple simultaneous breakup events, [F79](#)), such a scenario would lift the high mass requirement for the swarm progenitors, so that other candidates could be considered.

In that regard, Jupiter family comets (JFC) have been found via dynamical modelling to be able to produce also micrometeoroids on prograde orbits with very low semi-major axis and aphelia near 1 au, which would generate low-velocity near-apex meteor radiants ([Nesvorný et al., 2011](#)). As cometary meteoroids, which are generally associated with low bulk densities, these could constitute the missing meteoroid subpopulation, that produce the magnetospheric swarms. Moreover, their preferential approach direction from the Earth apex would be consistent with the swarms' apparent anisotropy. Quantitatively, their occurrence is expected to be only secondary to those from the likewise JFC-generated, higher-velocity helion/antihelion radiants ($\sim 30 \text{ km s}^{-1}$), as well as the yet-higher-velocity north/south apex radiants ($\sim 60 \text{ km s}^{-1}$) sustained by Halley-type and long-period comets ([Nesvorný et al., 2011](#)), which, however, might less readily produce swarms, due to their shorter residence times within the magnetosphere.

A population of grains that appear to exhibit similar dynamics has been detected in head-echo radar meteor with the Arecibo Observatory (AO). These slow meteors ($\sim 15 \text{ km s}^{-1}$) emerged when AO pointed near the Earth apex, alongside higher rates of fast meteors from the north/south apex radiants ([Janches et al., 2003](#); [Sulzer, 2004](#); [Janches and Chau, 2005](#)). The range of particle sizes constituting the AO dataset is stated to be $0.5\text{--}100 \mu\text{m}$, yet the sensitivity of head-echo radar meteor observations to slow particles $<30 \text{ km s}^{-1}$ has been a matter of debate and is likely closer to the higher end of the stated range ([Fentzke and Janches, 2008](#); [Janches et al., 2014, 2015, 2017](#)).

The dynamics of the swarms may hint at a connection to another group of interplanetary dust grains, namely, the α -meteoroids ([Grün and Zook, 1980](#); [Sommer, 2023](#)). These particles move on highly eccentric orbits with aphelia near 1 au, where they thus exhibit low heliocentric velocities. The Earth effectively overtakes these slow-moving particles, such that they appear to be coming from around the Earth apex with $v_\infty = 5\text{--}20 \text{ km s}^{-1}$. The α -meteoroids notably exhibit the dynamical properties demanded for swarm progenitors, that is, a preferred approach direction from the apex, as well as relative velocities below 20 km s^{-1} . Yet, these micron-sized particles are only about 1–2 orders of magnitude more massive than the swarm particles themselves.

3.1.5 Other explanations

At the time of the HEOS-2 mission, the phenomenon of SRM dust streams was not yet well-known, which is why they were not considered as explanation for the clusters in the interpretation of HEOS-2 data. As it was established that GEO-insertion SRM firings could create distinct dust formations in orbit around Earth, [Fechtig \(1984\)](#) acknowledged that they could be another explanation for the observed swarms. However, there are reasons why the HEOS-2-detected clusters are unlikely to be SRM exhaust dust formations, namely the altitude and the locations at which they occurred. The swarms were observed at all altitudes up to 60 000 km. In SRM GEO insertions, the exhaust dust is expelled rather retrograde such that the maximum obtainable apogee of ejected particles is near the GEO altitude (about 36 000 km) ([Mueller and Kessler, 1985](#); [Bunte, 2003](#)). On the other hand, the orbit of HEOS-2 was oriented such that the spacecraft reached its far-out apogee near the ecliptic north direction, causing it to spend only very limited time near the equatorial region. (see Figure 1). The north polar region was in use at the time by Russian Molniya satellites. However, those were launched by the Molniya-M launcher, which used a liquid upper stage (notwithstanding the fact that SRM dust ejected in Molniya orbit insertions would fail to reach a stable orbit).

It is conceivable that orbital perturbations could have caused SRM dust formations to drift from their origin region to where the swarms were observed. However, it is questionable whether these displacements could take place in the lifetimes of SRM dust streams, which are limited by atmospheric drag (at most 1–2 months for particles $<1 \mu\text{m}$ in size ([Friesen et al., 1992](#); [Bunte, 2003](#))). Moreover, electrodynamic perturbations on Earth-orbiting dust particles tend to dissipate their orbital energy, adding to the orbital decay due to atmospheric drag ([Juhász and Horányi, 1997](#)). Even if perturbations can meaningfully move GEO-insertion SRM dust to high altitude polar regions, their stochastic nature would arguably lead to the dispersion of the dust clouds.

Lastly, the Earth-apex anisotropy of the HEOS-2-detected swarms has no obvious explanation in the context of SRM dust, similarly to the preference of local midnight hours for cluster detections by GORID.

An entirely different explanation could be that the consistently detected clusters are not true particle impacts but rather

noise events caused by an interaction of the impact ionization detectors with the Earth’s magnetosphere. Spurious detections caused by various environmental factors have been a notorious issue for dust-counter-type instruments, requiring sophisticated data reduction techniques (e.g., [Poppe et al., 2011](#)), or invalidating datasets outright ([Nilsson, 1966](#)). In order to distinguish true impacts from noise events, a coincidence criterion was used with HEOS-2 and GORID, requiring valid successive charge signals from different measurement channels. With HEOS-2, a two-way coincidence criterion (target and ion collector) was used, which for instance, classified all events registered during a historically powerful solar storm of August 1972 as noise ([Dietzel et al., 1973](#)). GORID on the other hand, employed a three-way coincidence criterion (target charge, ion grid, and channeltron) to identify true impacts with considerable confidence ([Baguhl et al., 1993](#); [Grün et al., 1995](#)). (Note that GORID is identical to the Ulysses and Galileo detectors.) A significant amount of events classified by GORID as probably noise-induced appears to be linked to an electrostatic interaction with the spacecraft as well as to the operation of its plasma thrusters, as described in ([Drolshagen et al., 2001a](#)). Note that usually only the highest-confidence true-impact events have been used in the referred-to analyses of the GORID data. Nevertheless, it is at least conceivable that a so-far unknown interaction of the impact-ionization-type detectors with the magnetosphere’s turbulent plasma environment may cause the clustered occurrence of genuine-looking noise events, despite the scrutiny put in place. Given that electromagnetic effects are evidently conducive to the occurrence of noise events, the apparent correlation of cluster detections with geomagnetic activity (Section 3.1.2) is arguably consistent with that proposition.

3.2 Future investigation with DESTINY+

JAXA’s DESTINY+ mission is a planned small body science mission to active asteroid 3200 Phaethon, scheduled for launch in 2025. It carries the DESTINY+ Dust Analyzer (DDA), a state-of-the-art dust detector that allows for the simultaneous analysis of particles’ dynamical (via charge-sensitive entry grids) and compositional (via an impact plasma mass spectrometer) information ([Simolka and et al., 2024](#)). In addition to studying the dust environment of Phaethon, DDA will conduct science operations during the entire nominal mission duration of 3 years, to study interplanetary and interstellar dust ([Krüger et al., 2019](#)). For the first two years of the mission, the spacecraft revolves in Earth-bound orbits, during which it gradually ascends from an initially GTO-like orbit all the way to the Moon’s orbit using its solar electric propulsion system, as shown in Figure 4. Eventually, DESTINY+ will conduct a series of lunar gravity assists to escape the Earth-Moon system and further advance towards Phaethon.

DDA will thus have extensive exposure to the near-Earth dust environment at all altitudes beyond LEO. DESTINY+ will pass through the magnetosphere at altitudes $< 10 R_{\oplus}$ for roughly the first year of the mission, and then traverse the plasma sheet region for several more months after that. Unlike HEOS-2, DESTINY+ will remain within equatorial rather than the polar regions of the magnetosphere, at an orbital inclination of $\sim 31^{\circ}$. The near-Earth mission phase of the mission will coincide with the solar cycle 25 maximum, which is expected for mid 2025.

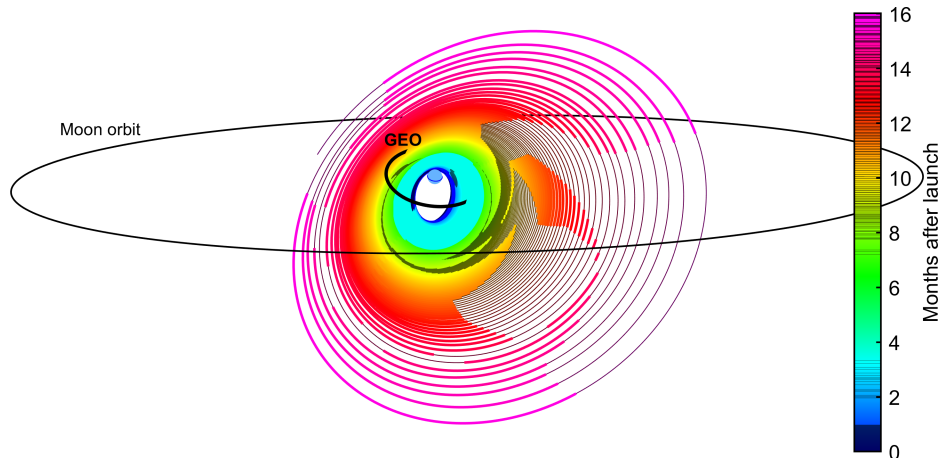


Figure 4: Trajectory of the initial phase of the DESTINY+ mission, during which the spacecraft will gradually raise its orbit towards the Moon. Phases of thrusting and coasting are indicated by thick and thin lines, respectively.

The DESTINY+ mission profile combined with the capabilities of the DDA instrument represent a unique opportunity to further investigate the clustering phenomena previously reported by HEOS-2 and GORID. By recording a valid mass spectrum

of a particle’s impact plasma, DDA can unequivocally identify true particle impacts. It could thus rule out the possibility of the clusters being spurious noise events. The compositional analysis of swarm particles—should they be found—would then give definitive proof of their natural or artificial origin. Moreover, DDA’s charge-sensing entrance grids may register larger swarm particles (reported by HEOS-2 to have masses up to 10^{-11} g (F79), corresponding to sizes of roughly ~ 1 μm), allowing for a direct measurement of their charge and velocity. Such measurements would undoubtedly be crucial for understanding the swarms’ formation mechanism.

Similarly to how we related the incidence rates of HEOS-2 and GORID to each other, we may tentatively estimate the incidence rate of swarm particles onto DDA by converting the HEOS-2 and GORID rates (see Section 3.1.3) to DDA rates using the relation of their respective geometrical factors (see Table 1). This yields 133 swarm particle impacts per month onto DDA according to HEOS-2 rates and 4.2 impacts per months according to GORID rates (for the time within the magnetosphere). Identifying the reason(s) for this discrepancy (as speculated upon in Section 3.1.3) would be a key aspect of the investigation. It’s important to note that this simple calculation ignores the differences in spacecraft orbits and instrument pointings.

4 Conclusion

We have provided an overview of the various reports of clustered impact events given by dust-counter-type instruments in near-Earth space. The clustered impacts detected by the HEOS-2 and GORID impact ionization detectors within the magnetosphere and at GEO, respectively, represent a peculiar phenomenon, which have been interpreted as transient particle swarms created either by the breakup of meteoroids, or by GEO spaceflight activities. We have assessed the possibility that the swarms observed by both instruments are caused by the same phenomenon, which is indicated by commonalities regarding their encounter durations and their anisotropy. Remarkably, we have found that in both cases their occurrence was correlated with high geomagnetic activity, which is consistent with the notion that the swarms are caused by the electrostatic breakup of meteoroids proposed by F79, but could also be interpreted as in favour of the clusters being spurious, plasma-environment-induced noise events. While the GORID-detected clusters might also stem from the electrostatic breakup of SRM slag particles in GTO-like orbits (as speculated by Graps et al., 2007), this scenario can hardly explain the HEOS-2-detected swarms, which were observed far from the equatorial plane and at altitudes of up to 60 000 km.

Lacking the proper dynamical and compositional characterization of dust particles—which both HEOS-2 and GORID were unable to provide—the nature of the swarms remains elusive. The upcoming DESTINY+ mission, however, will carry a sophisticated dust analyser instrument (the DDA), which will offer these capabilities. Considering the mission’s prolonged orbit raising phase through the magnetosphere, DESTINY+/DDA poses a unique opportunity to finally unveil the origin of the putative particle swarms.

In light of the new insights presented here, it may be worth to revisit in particular the GORID data, and analyse the timings and locations of cluster detections more thoroughly with respect to geomagnetic activity and region within the magnetosphere. Exploring dust counter data retrieved from the magnetospheres of Jupiter and Saturn for similar swarms could provide additional avenue for investigating this phenomenon. While most observed clusters there were linked to dynamic nano-dust streams from the moons Io and Enceladus, there have also been reports of impact clusters of unresolved origin seen by the Cassini Cosmic Dust Analyzer (CDA) in orbit around Saturn (Hsu et al., 2011).

Finally, new insights about electrostatic effects in cosmic dust, in particular the ‘electrostatic lofting’ of grains from dusty surfaces suspended in a plasma or UV light (e.g., Wang et al., 2016), could help shed light on the formation mechanism of the magnetospheric swarms.

Acknowledgement

I thank Simon Green and Tony McDonnell for their assistance in acquiring valuable literature about the GORID results, as well as three anonymous reviewers for their constructive comments. Partial support by the German Aerospace Center (DLR, grant no. 50002101) is gratefully acknowledged.

References

- Akiba, R., Inatani, Y., 1990. Alumina Particles Exhausted from Solid-Propellant Rocket Motor As a Potential Source of Space Debris, in: ISAS Science Report SP 11 - Proceedings of the Workshop on Space Debris, pp. 51–59. URL: <https://cir.nii.ac.jp/crid/1050003824960878592>.
- Altobelli, N., Krüger, H., Moissl, R., Landgraf, M., Grün, E., 2004. Influence of wall impacts on the Ulysses dust detector on understanding the interstellar dust flux. *Planetary and Space Science* 52, 1287–1295. URL: <https://www.sciencedirect.com/science/article/pii/S0032063304001163>, doi:10.1016/j.pss.2004.07.022.
- Baguhl, M., Grün, E., Linkert, G., Linkert, D., Siddique, N., 1993. Identification of “small” dust impacts in the Ulysses dust detector data. *Planetary and Space Science* 41, 1085–1098. URL: <https://www.sciencedirect.com/science/article/pii/S003206339390112F>, doi:10.1016/0032-0633(93)90112-F.
- Baker, D.N., Li, X., Blake, J.B., Kanekal, S., 1998. Strong electron acceleration in the Earth’s magnetosphere. *Advances in Space Research* 21, 609–613. URL: <https://www.sciencedirect.com/science/article/pii/S0273117797009708>, doi:10.1016/S0273-1177(97)00970-8.
- Bedford, D.K., Adams, N.G., Smith, D., 1975a. The flux and spatial distribution of micrometeoroids in the near-Earth environment. *Planetary and Space Science* 23, 1451–1456. URL: <https://www.sciencedirect.com/science/article/pii/S0032063375900410>, doi:10.1016/0032-0633(75)90041-0.
- Bedford, D.K., Massey, H.S.W., Dalziel, R., King-Hele, D.G., 1975b. Observations of the micrometeoroid flux from Prospero. *Proceedings of the Royal Society of London. A. Mathematical and Physical Sciences* 343, 277–287. URL: <https://royalsocietypublishing.org/doi/abs/10.1098/rspa.1975.0065>, doi:10.1098/rspa.1975.0065.
- Bedford, D.K., Sayers, J., 1973. The near earth micrometeoroid flux from the satellite Prospero, in: *Space Research XIII, Proceedings of the Open Meetings of the Working Groups on Physical Sciences of the 15th Plenary Meeting of COSPAR*, pp. 1063–1069. URL: <https://ui.adsabs.harvard.edu/abs/1973spre.conf.1063B>.
- Boynton, R.J., Balikhin, M.A., Billings, S.A., Reeves, G.D., Ganushkina, N., Gedalin, M., Amariutei, O.A., Borovsky, J.E., Walker, S.N., 2013. The analysis of electron fluxes at geosynchronous orbit employing a NARMAX approach. *Journal of Geophysical Research: Space Physics* 118, 1500–1513. URL: <https://onlinelibrary.wiley.com/doi/abs/10.1002/jgra.50192>, doi:10.1002/jgra.50192.
- Bunte, K.D., 2003. The Detectability of Debris Particle Clouds, in: *54th IAC of the IAF*, pp. IAA–5.1.07. URL: <https://arc.aiaa.org/doi/abs/10.2514/6.IAC-03-IAA.5.1.07>, doi:10.2514/6.IAC-03-IAA.5.1.07.
- Bunte, K.D., Drolshagen, G., 2005. Detection and Simulation of Debris Cloud Impacts, in: *ESA SP-587*, p. 201. URL: <https://ui.adsabs.harvard.edu/abs/2005ESASP.587..201B/abstract>.
- Bunte, K.D., Graps, A.L., Green, S.F., Kuitunen, J., McBride, N., McDonnell, J.A.M., Schwanethal, J., Timme, M., 2006. Processing, Analysis and Interpretation of Data from Impact Detector. Technical Report Final Report of ESA contr. 16272/02/NL/EC.
- Ceplecha, Z., 1977. Meteoroid Populations and Orbits, in: *IAU Colloquium 39*, pp. 143–152. URL: <https://www.cambridge.org/core/journals/international-astronomical-union-colloquium/article/5-meteoroid-populations-and-orbits/EC4EA5650C0046FC056B7225A8275785>, doi:10.1017/S0252921100070044.
- Ceplecha, Z., Borovička, J., Elford, W.G., ReVelle, D.O., Hawkes, R.L., Porubčan, V., Šimek, M., 1998. Meteor Phenomena and Bodies. *Space Science Reviews* 84, 327–471. URL: <https://doi.org/10.1023/A:1005069928850>, doi:10.1023/A:1005069928850.
- Cooke, W.J., Oliver, J.P., Simon, C.G., 1995. The orbital characteristics of debris particle rings as derived from IDE observations of multiple orbit intersections with LDEF, in: *LDEF: 69 Months in Space. Third Post-Retrieval Symposium, Part 1*, pp. 361–371. URL: <https://ntrs.nasa.gov/citations/19950017409>.
- Dietzel, H., Eichhorn, G., Fechtig, H., Grün, E., Hoffmann, H.J., Kissel, J., 1973. The HEOS 2 and HELIOS micrometeoroid experiments. *Journal of Physics E: Scientific Instruments* 6, 209–217. URL: <https://iopscience.iop.org/article/10.1088/0022-3735/6/3/008>, doi:10.1088/0022-3735/6/3/008.
- Dohnanyi, J.S., 1972. Interplanetary objects in review: Statistics of their masses and dynamics. *Icarus* 17, 1–48. URL: <https://www.sciencedirect.com/science/article/pii/0019103572900449>, doi:10.1016/0019-1035(72)90044-9.
- Dohnanyi, J.S., 1977. Groups of micrometeoroids in the Earth-Moon system, in: *Space Research XVII, Proceedings of the Open Meetings of Working Groups on Physical Sciences*, pp. 623–625. URL: <https://ui.adsabs.harvard.edu/abs/1977spre.conf..623D>.

- Dohnanyi, J.S., Fechtig, H., 1977. Micrometeoroid swarms, in: Space Research XVII, Proceedings of the Open Meetings of Working Groups on Physical Sciences, pp. 571–572. URL: <https://ui.adsabs.harvard.edu/abs/1977spre.conf..571D>.
- Drolshagen, G., 2006. In-situ Observations of Space Debris at ESA, in: Advanced Maui Optical and Space Surveillance Technologies Conference, p. E68. URL: -.
- Drolshagen, G., Svedhem, H., Grün, E., 2001a. Measurements of cosmic dust and micro-debris with the GORID impact detector in GEO, in: Proceedings of the Third European Conference on Space Debris (ESA SP-473), pp. 177–184. URL: <https://ui.adsabs.harvard.edu/abs/2001ESASP.473..177D>.
- Drolshagen, G., Svedhem, H., Grün, E., Bunte, K.D., 2001b. Measurements of cosmic dust and micro-debris in GEO. *Advances in Space Research* 28, 1325–1333. URL: <https://www.sciencedirect.com/science/article/pii/S0273117701004057>, doi:10.1016/S0273-1177(01)00405-7.
- Drolshagen, G., Svedhem, H., Grün, E., Grafodatsky, O., Prokopiev, U., 1999. Microparticles in the geostationary orbit (GORID experiment). *Advances in Space Research* 23, 123–133. URL: <https://www.sciencedirect.com/science/article/pii/S0273117798002397>, doi:10.1016/S0273-1177(98)00239-7.
- Durin, C., Mandeville, J.C., 2009. SODAD: First results and post-flight analysis, in: Proceedings of ISMSE. URL: http://esmat.esa.int/materials_news/isme09/pdf/10-In-flight/S12%20-%20Durin.pdf.
- Durin, C., Mandeville, J.C., Perrin, J.M., 2016. System for an Active Detection of Orbital Debris in Space. *Journal of Spacecraft and Rockets* 53, 1178–1184. URL: <https://doi.org/10.2514/1.A33455>, doi:10.2514/1.A33455.
- Durin, Ch., Mandeville, J.C., Perrin, J.M., 2022. Active detection of micrometeoroids and space debris SODAD-2 experiment on SAC-D satellite. *Advances in Space Research* 69, 3856–3863. URL: <https://www.sciencedirect.com/science/article/pii/S0273117722001570>, doi:10.1016/j.asr.2022.02.045.
- Fechtig, H., 1984. The interplanetary dust environment beyond 1 AU and in the vicinity of the ringed planets (tutorial talk). *Advances in Space Research* 4, 5–11. URL: <https://www.sciencedirect.com/science/article/pii/0273117784900024>, doi:10.1016/0273-1177(84)90002-4.
- Fechtig, H., Grün, E., Morfill, G., 1979. Micrometeoroids within ten Earth radii. *Planetary and Space Science* 27, 511–531. URL: <https://www.sciencedirect.com/science/article/pii/0032063379901284>, doi:10.1016/0032-0633(79)90128-4.
- Fechtig, H., Hemenway, C., 1976. Near-earth fragmentation of cosmic dust, in: IAU Colloquium 31, Interplanetary Dust and Zodiacal Light, pp. 290–295. URL: https://doi.org/10.1007/3-540-07615-8_497, doi:10.1007/3-540-07615-8_497.
- Fentzke, J.T., Janches, D., 2008. A semi-empirical model of the contribution from sporadic meteoroid sources on the meteor input function in the MLT observed at Arecibo. *Journal of Geophysical Research: Space Physics* 113. URL: <https://onlinelibrary.wiley.com/doi/abs/10.1029/2007JA012531>, doi:10.1029/2007JA012531.
- Friedel, R.H.W., Reeves, G.D., Obara, T., 2002. Relativistic electron dynamics in the inner magnetosphere — a review. *Journal of Atmospheric and Solar-Terrestrial Physics* 64, 265–282. URL: <https://www.sciencedirect.com/science/article/pii/S1364682601000888>, doi:10.1016/S1364-6826(01)00088-8.
- Friesen, L.J., Jackson, A.A., Zook, H.A., Kessler, D.J., 1992. Results in orbital evolution of objects in the geosynchronous region. *Journal of Guidance, Control, and Dynamics* 15, 263–267. URL: <https://arc.aiaa.org/doi/10.2514/3.20827>, doi:10.2514/3.20827.
- Göller, J., Grün, E., 1989. Calibration of the Galileo/Ulysses dust detectors with different projectile materials and at varying impact angles. *Planetary and Space Science* 37, 1197–1206. URL: <https://linkinghub.elsevier.com/retrieve/pii/0032063389900147>, doi:10.1016/0032-0633(89)90014-7.
- Gosling, J.T., Asbridge, J.R., Bame, S.J., 1977. An unusual aspect of solar wind speed variations during solar cycle 20. *Journal of Geophysical Research (1896-1977)* 82, 3311–3314. URL: <https://onlinelibrary.wiley.com/doi/abs/10.1029/JA082i022p03311>, doi:10.1029/JA082i022p03311.
- Graham, G.A., Kearsley, A.T., Drolshagen, G., McBride, N., Green, S.F., Wright, I.P., 2001. Microparticle impacts upon HST solar cells. *Advances in Space Research* 28, 1341–1346. URL: <https://www.sciencedirect.com/science/article/pii/S0273117701004082>, doi:10.1016/S0273-1177(01)00408-2.
- Graps, A., Grün, E., 2000. Properties, Charging, and Dynamics of Interplanetary Dust Particles in Earth’s Magnetosphere. Technical Report ESA Contract 13145/98.

- Graps, A.L., Green, S.F., McBride, N., McDonnell, J.A.M., Bunte, K., Svedhem, H., Drolshagen, G., 2007. GEO Debris and Interplanetary Dust: Fluxes and Charging Behavior, in: ESA SP-643, pp. 97–102. URL: <https://ui.adsabs.harvard.edu/abs/2007ESASP.643...97G>.
- Grün, E., Baguhl, M., Hamilton, D.P., Kissel, J., Linkert, D., Linkert, G., Riemann, R., 1995. Reduction of Galileo and Ulysses dust data. *Planetary and Space Science* 43, 941–951. URL: <https://www.sciencedirect.com/science/article/pii/003206339400232G>, doi:10.1016/0032-0633(94)00232-G.
- Grün, E., Fechtig, H., Hanner, M.S., Kissel, J., Lindblad, B.A., Linkert, D., Maas, D., Morfill, G.E., Zook, H.A., 1992a. The Galileo Dust Detector. *Space Science Reviews* 60, 317–340. URL: <https://doi.org/10.1007/BF00216860>, doi:10.1007/BF00216860.
- Grün, E., Fechtig, H., Kissel, J., Linkert, D., Maas, D., McDonnell, J.A.M., Morfill, G.E., Schwehm, G., Zook, H.A., Giese, R.H., 1992b. The Ulysses dust experiment. *Astronomy and Astrophysics Supplement Series* 92, 411–423. URL: <https://ui.adsabs.harvard.edu/abs/1992A&AS...92..411G/abstract>.
- Grün, E., Zook, H.A., 1980. Dynamics of Micrometeoroids, in: *IAU Symposium*, pp. 293–298. URL: <https://www.cambridge.org/core/journals/symposium-international-astronomical-union/article/dynamics-of-micrometeoroids/C8C8B03CFBEF33CA3F7D4ACE6A40B525>, doi:10.1017/S0074180900066912.
- Hill, J.R., Mendis, D.A., 1981. Electrostatic disruption of a charged conducting spheroid. *Canadian Journal of Physics* 59, 897–901. URL: <https://cdnsiencepub.com/doi/10.1139/p81-116>, doi:10.1139/p81-116.
- Hoffmann, H.J., Fechtig, H., Grün, E., Kissel, J., 1975a. First results of the micrometeoroid experiment s 215 on the HEOS 2 satellite. *Planetary and Space Science* 23, 215–224. URL: <https://linkinghub.elsevier.com/retrieve/pii/003206337590080X>, doi:10.1016/0032-0633(75)90080-X.
- Hoffmann, H.J., Fechtig, H., Grün, E., Kissel, J., 1975b. Temporal fluctuations and anisotropy of the micrometeoroid flux in the Earth-Moon system measured by HEOS 2. *Planetary and Space Science* 23, 985–991. URL: <https://www.sciencedirect.com/science/article/pii/0032063375901865>, doi:10.1016/0032-0633(75)90186-5.
- Horányi, M., 1996. Charged Dust Dynamics in the Solar System. *Annual Review of Astronomy and Astrophysics* 34, 383–418. URL: <https://doi.org/10.1146/annurev.astro.34.1.383>, doi:10.1146/annurev.astro.34.1.383.
- Hörz, F., Bernhard, R., See, T., Kessler, D., 2002. Metallic and Oxidized Aluminum Debris Impacting the Trailing Edge of the Long Duration Exposure Facility (LDEF). *Space Debris* 2, 51–66. URL: <https://doi.org/10.1023/A:1015689229412>, doi:10.1023/A:1015689229412.
- Hsu, H.W., Kempf, S., Postberg, F., Trieloff, M., Burton, M., Roy, M., Moragas-Klostermeyer, G., Srama, R., 2011. Cassini dust stream particle measurements during the first three orbits at Saturn. *Journal of Geophysical Research: Space Physics* 116. URL: <https://onlinelibrary.wiley.com/doi/abs/10.1029/2010JA015959>, doi:10.1029/2010JA015959.
- Iglseder, H., Grün, E., Münzenmayer, R., Svedhem, H., 1993a. Analysis of the results of two-year operations of the Munich Dust Counter - a cosmic dust experiment on board the satellite HITEN, in: *IAU Symposium*, p. 377. URL: <https://ui.adsabs.harvard.edu/abs/1993mtpb.conf..377I>.
- Iglseder, H., Münzenmayer, R., Svedhem, H., Grün, E., 1993b. Cosmic dust and space debris measurements with the Munich dust counter on board the satellites hiten and brem-sat. *Advances in Space Research* 13, 129–132. URL: <https://linkinghub.elsevier.com/retrieve/pii/027311779390579Z>, doi:10.1016/0273-1177(93)90579-Z.
- Jackson, A., Eichler, P., Potter, R.R.A., Johnson, N., 1997. The Historical Contribution of Solid Rocket Motors to the One Centimeter Debris Population, in: *Proceedings of the 2nd European Conference on Space Debris*, ESA-SP 393, p. 279. URL: <https://ui.adsabs.harvard.edu/abs/1997ESASP.393..279J>.
- Janches, D., Chau, J.L., 2005. Observed diurnal and seasonal behavior of the micrometeor flux using the Arecibo and Jicamarca radars. *Journal of Atmospheric and Solar-Terrestrial Physics* 67, 1196–1210. URL: <https://www.sciencedirect.com/science/article/pii/S1364682605001227>, doi:10.1016/j.jastp.2005.06.011.
- Janches, D., Nolan, M.C., Meisel, D.D., Mathews, J.D., Zhou, Q.H., Moser, D.E., 2003. On the geocentric micrometeor velocity distribution. *Journal of Geophysical Research: Space Physics* 108. URL: <https://onlinelibrary.wiley.com/doi/abs/10.1029/2002JA009789>, doi:10.1029/2002JA009789.
- Janches, D., Plane, J.M.C., Nesvorný, D., Feng, W., Vokrouhlický, D., Nicolls, M.J., 2014. RADAR DETECTABILITY STUDIES OF SLOW AND SMALL ZODIACAL DUST CLOUD PARTICLES. I. THE CASE OF ARECIBO 430 MHz METEOR HEAD ECHO OBSERVATIONS. *The Astrophysical Journal* 796, 41. URL: <https://dx.doi.org/10.1088/0004-637X/796/1/41>, doi:10.1088/0004-637X/796/1/41.

- Janches, D., Swarnalingam, N., Carrillo-Sanchez, J.D., Gomez-Martin, J.C., Marshall, R., Nesvorný, D., Plane, J.M.C., Feng, W., Pokorný, P., 2017. Radar Detectability Studies of Slow and Small Zodiacal Dust Cloud Particles. III. The Role of Sodium and the Head Echo Size on the Probability of Detection. *The Astrophysical Journal* 843, 1. URL: <https://dx.doi.org/10.3847/1538-4357/aa775c>, doi:10.3847/1538-4357/aa775c.
- Janches, D., Swarnalingam, N., Plane, J.M.C., Nesvorný, D., Feng, W., Vokrouhlický, D., Nicolls, M.J., 2015. RADAR DETECTABILITY STUDIES OF SLOW AND SMALL ZODIACAL DUST CLOUD PARTICLES. II. A STUDY OF THREE RADARS WITH DIFFERENT SENSITIVITY. *The Astrophysical Journal* 807, 13. URL: <https://dx.doi.org/10.1088/0004-637X/807/1/13>, doi:10.1088/0004-637X/807/1/13.
- Juhász, A., Horányi, M., 1997. Dynamics of charged space debris in the Earth's plasma environment. *Journal of Geophysical Research: Space Physics* 102, 7237–7246. URL: <https://onlinelibrary.wiley.com/doi/abs/10.1029/96JA03672>, doi:10.1029/96JA03672.
- Kessler, D.J., 1991. Collisional cascading: The limits of population growth in low earth orbit. *Advances in Space Research* 11, 63–66. URL: <https://www.sciencedirect.com/science/article/pii/027311779190543S>, doi:10.1016/0273-1177(91)90543-S.
- Kessler, D.J., Su, S.Y. (Eds.), 1985. *Orbital Debris*. NASA-CP-2360. URL: <https://ntrs.nasa.gov/citations/19850012878>. proceedings of a workshop sponsored by NASA Lyndon B. Johnson Space Center and held in Houston, Texas.
- Krüger, H., Strub, P., Srama, R., Kobayashi, M., Arai, T., Kimura, H., Hirai, T., Moragas-Klostermeyer, G., Altobelli, N., Sterken, V.J., Agarwal, J., Sommer, M., Grün, E., 2019. Modelling DESTINY+ interplanetary and interstellar dust measurements en route to the active asteroid (3200) Phaethon. *Planetary and Space Science* 172, 22–42. URL: <https://linkinghub.elsevier.com/retrieve/pii/S0032063318303647>, doi:10.1016/j.pss.2019.04.005.
- Laurance, M.R., Brownlee, D.E., 1986. The flux of meteoroids and orbital space debris striking satellites in low Earth orbit. *Nature* 323, 136–138. URL: <https://www.nature.com/articles/323136a0>, doi:10.1038/323136a0.
- Matzka, J., Bronkalla, O., Tornow, K., Elger, K., Stolle, C., 2021a. Geomagnetic Kp index, V. 1.0. GFZ Data Services doi:10.5880/Kp.0001.
- Matzka, J., Stolle, C., Yamazaki, Y., Bronkalla, O., Morschhauser, A., 2021b. The Geomagnetic Kp Index and Derived Indices of Geomagnetic Activity. *Space Weather* 19, e2020SW002641. URL: <https://onlinelibrary.wiley.com/doi/abs/10.1029/2020SW002641>, doi:10.1029/2020SW002641.
- McDonnell, J.A.M., 1978. Microparticle studies by space instrumentation, in: *Cosmic Dust*, pp. 337–426. URL: <https://ui.adsabs.harvard.edu/abs/1978codu.book..337M>.
- McDowel, J., 1997. Kick in the apogee - 40 years of upper stage applications for solid rocket motors, 1957-1997, in: 33rd Joint Propulsion Conference and Exhibit. URL: <https://arc.aiaa.org/doi/abs/10.2514/6.1997-3133>, doi:10.2514/6.1997-3133.
- Mendis, D.A., 1981. The role of electrostatic charging of small and intermediate sized bodies in the solar system, in: *Investigating the Universe: Papers Presented to Zdeněk Kopal on the Occasion of His Retirement, September 1981*. Springer Netherlands. Astrophysics and Space Science Library, pp. 353–384. URL: https://doi.org/10.1007/978-94-009-8534-6_12, doi:10.1007/978-94-009-8534-6_12.
- Mendis, D.A., 1984. Entry of dust particles into planetary magnetospheres. *Advances in Space Research* 4, 111–120. URL: <https://www.sciencedirect.com/science/article/pii/0273117784900152>, doi:10.1016/0273-1177(84)90015-2.
- Menicucci, A., Drolshagen, G., Kuitunen, J., Butenko, Y., Mooney, C., 2013. In-Flight and Post-Flight Impact Data Analysis from DEBIE2 (Debris In-Orbit Evaluator) on Board of ISS, in: *Proceedings of the 6th European Conference on Space Debris*. URL: <https://conference.sdo.esoc.esa.int/proceedings/sdc6/paper/185>.
- Mueller, A.C., Kessler, D.J., 1985. The effects of particulates from solid rocket motors fired in space. *Advances in Space Research* 5, 77–86. URL: <https://www.sciencedirect.com/science/article/pii/0273117785903898>, doi:10.1016/0273-1177(85)90389-8.
- Neish, M., Goka, T., Imagawa, K., 2004. Numerical Analysis of a Debris Swarm of Solid Rocket Motor Dust Particles, in: 35th COSPAR Scientific Assembly, p. 1794. URL: <https://ui.adsabs.harvard.edu/abs/2004cosp...35.1794N>.
- Nesvorný, D., Janches, D., Vokrouhlický, D., Pokorný, P., Bottke, W.F., Jenniskens, P., 2011. DYNAMICAL MODEL FOR THE ZODIACAL CLOUD AND SPORADIC METEORS. *The Astrophysical Journal* 743, 129. URL: <https://iopscience.iop.org/article/10.1088/0004-637X/743/2/129>, doi:10.1088/0004-637X/743/2/129.

- Nilsson, C., 1966. Some Doubts about the Earth's Dust Cloud. *Science* 153, 1242–1246. URL: <https://www.science.org/doi/abs/10.1126/science.153.3741.1242>, doi:10.1126/science.153.3741.1242.
- Oliver, J.P., Singer, S.F., Weinberg, J.L., Simon, C.G., Cooke, W.J., Kassel, P.C., Kinard, W.H., Mulholland, J.D., Wortman, J.J., 1995. LDEF Interplanetary Dust Experiment (IDE) results. URL: <https://ntrs.nasa.gov/citations/19950017408>.
- Öpik, E.J., 1956. Interplanetary Dust and Terrestrial Accretion of Meteoric Matter. *Irish Astronomical Journal* 4, 84. URL: <https://ui.adsabs.harvard.edu/abs/1956IrAJ....4...84O>.
- Poppe, A., James, D., Horányi, M., 2011. Measurements of the terrestrial dust influx variability by the Cosmic Dust Experiment. *Planetary and Space Science* 59, 319–326. URL: <https://www.sciencedirect.com/science/article/pii/S0032063310003624>, doi:10.1016/j.pss.2010.12.002.
- Reeves, G.D., Morley, S.K., Friedel, R.H.W., Henderson, M.G., Cayton, T.E., Cunningham, G., Blake, J.B., Christensen, R.A., Thomsen, D., 2011. On the relationship between relativistic electron flux and solar wind velocity: Paulikas and Blake revisited. *Journal of Geophysical Research: Space Physics* 116. URL: <https://onlinelibrary.wiley.com/doi/abs/10.1029/2010JA015735>, doi:10.1029/2010JA015735.
- Richardson, I.G., Cane, H.V., 2012. Solar wind drivers of geomagnetic storms during more than four solar cycles. *Journal of Space Weather and Space Climate* 2, A01. URL: <https://www.swsc-journal.org/articles/swsc/abs/2012/01/swsc120012/swsc120012.html>, doi:10.1051/swsc/2012001.
- Richardson, I.G., Cliver, E.W., Cane, H.V., 2000. Sources of geomagnetic activity over the solar cycle: Relative importance of coronal mass ejections, high-speed streams, and slow solar wind. *Journal of Geophysical Research: Space Physics* 105, 18203–18213. URL: <https://onlinelibrary.wiley.com/doi/abs/10.1029/1999JA000400>, doi:10.1029/1999JA000400.
- Schobert, D., Paul, K.G., 1997. Al₂O₃ particle fluxes from the ECS 2 apogee maneuver—Witnessed by the LDEF interplanetary dust experiment. *Advances in Space Research* 19, 271–274. URL: <https://www.sciencedirect.com/science/article/pii/S0273117797000185>, doi:10.1016/S0273-1177(97)00018-5.
- Schwanethal, J.P., McBride, N., Green, S.F., McDonnell, J.A.M., Drolshagen, G., 2005. Analysis of Impact Data from the Debris (debris In-Orbit Evaluator) Sensor in Polar Low Earth Orbit, in: *Proceedings of the 4th European Conference on Space Debris*, ESA SP-587, p. 177. URL: <https://conference.sdo.esoc.esa.int/proceedings/sdc4/paper/102>.
- Simolka, J., et al., 2024. The DESTINY+ Dust Analyser - a dust telescope for analysing cosmic dust dynamics and composition. *Philosophical Transactions of the Royal Society A* this issue.
- Singer, S.F., Stanley, J.E., 1980. Submicron Particles in Meteor Streams, in: *Properties and Interactions of Interplanetary Dust*, Proc. of IAU Symposium 90, pp. 329–332. URL: <https://www.cambridge.org/core/journals/symposium-international-astronomical-union/article/submicron-particles-in-meteor-streams/DF4D2AC262ABC50450A4BD160E55810B>, doi:10.1017/S0074180900067012.
- Sommer, M., 2023. Alpha-Meteoroids then and now: Unearthing an overlooked micrometeoroid population. *Planetary and Space Science* 236, 105751. URL: <https://www.sciencedirect.com/science/article/pii/S0032063323001204>, doi:10.1016/j.pss.2023.105751.
- Sommer, M., 2024. Science Planning for the DESTINY+ Dust Analyzer: Leveraging the Potential of a Space Exploration Instrument. Ph.D. thesis. University of Stuttgart. URL: <http://elib.uni-stuttgart.de/handle/11682/13910>.
- Stabroth, S., Homeister, M., Oswald, M., Wiedemann, C., Klinkrad, H., Vörsmann, P., 2008. The influence of solid rocket motor retro-burns on the space debris environment. *Advances in Space Research* 41, 1054–1062. URL: <https://www.sciencedirect.com/science/article/pii/S0273117706007824>, doi:10.1016/j.asr.2006.12.024.
- Stabroth, S., Oswald, M., Wiedemann, C., Klinkrad, H., Vörsmann, P., 2007. Explanation of the “May Swarm” signature in the LDEF IDE impact data. *Aerospace Science and Technology* 11, 253–257. URL: <https://www.sciencedirect.com/science/article/pii/S1270963807000144>, doi:10.1016/j.ast.2007.02.003.
- Stübig, M., 2002. New Insights in Impact Ionization and in Time-Of-Flight Mass Spectroscopy With Micrometeoroid Detectors by Improved Impact Simulations in the Laboratory. Ph.D. thesis. Heidelberg University. URL: <https://ui.adsabs.harvard.edu/abs/2002PhDT.....368S/abstract>, doi:10.11588/heidok.00003068.
- Sulzer, M.P., 2004. Meteoroid velocity distribution derived from head echo data collected at Arecibo during regular world day observations. *Atmospheric Chemistry and Physics* 4, 947–954. URL: <https://acp.copernicus.org/articles/4/947/2004/>, doi:10.5194/acp-4-947-2004.

- Tuzzolino, A., Economou, T., McKibben, R., Simpson, J., BenZvi, S., Blackburn, L., Voss, H., Gursky, H., 2005. Final results from the space dust (SPADUS) instrument flown aboard the earth-orbiting ARGOS spacecraft. *Planetary and Space Science* 53, 903–923. URL: <https://linkinghub.elsevier.com/retrieve/pii/S0032063305000772>, doi:10.1016/j.pss.2005.03.008.
- Tuzzolino, A.J., McKibben, R.B., Simpson, J.A., BenZvi, S., Voss, H.D., Gursky, H., Johnson, N.L., 2001. In-Situ Detections of a Satellite Breakup by the SPADUS Experiment, in: *Proceedings of the 3rd European Conference on Space Debris*, ESA SP-473, pp. 203–210. URL: <https://ntrs.nasa.gov/citations/20100029880>.
- Wang, X., Schwan, J., Hsu, H.W., Grün, E., Horányi, M., 2016. Dust charging and transport on airless planetary bodies. *Geophysical Research Letters* 43, 6103–6110. URL: <https://onlinelibrary.wiley.com/doi/abs/10.1002/2016GL069491>, doi:10.1002/2016GL069491.
- Wegener, P., Bendisch, J., Krag, H., Oswald, M., Stabroth, S., 2004. Population evolution in the GEO vicinity. *Advances in Space Research* 34, 1171–1176. URL: <https://www.sciencedirect.com/science/article/pii/S0273117704000985>, doi:10.1016/j.asr.2003.11.013.
- Wehry, A., Mann, I., 1999. Identification of β -meteoroids from measurements of the dust detector onboard the ULYSSES spacecraft. *Astronomy and Astrophysics* 341, 296–303. URL: <https://ui.adsabs.harvard.edu/abs/1999A&A...341..296W/abstract>.
- Willis, M.J., Burchell, M.J., Ahrens, T.J., Krüger, H., Grün, E., 2005. Decreased values of cosmic dust number density estimates in the Solar System. *Icarus* 176, 440–452. URL: <https://www.sciencedirect.com/science/article/pii/S0019103505000862>, doi:10.1016/j.icarus.2005.02.018.
- Willis, M.J., Burchell, M.J., Cole, M.J., McDonnell, J.A.M., 2004. Influence of impact ionisation detection methods on determination of dust particle flux in space. *Planetary and Space Science* 52, 711–725. URL: <https://www.sciencedirect.com/science/article/pii/S0032063304000170>, doi:10.1016/j.pss.2004.01.001.
- Zimbardo, G., Greco, A., Sorriso-Valvo, L., Perri, S., Vörös, Z., Aburjania, G., Chergazia, K., Alexandrova, O., 2010. Magnetic Turbulence in the Geospace Environment. *Space Science Reviews* 156, 89–134. URL: <https://doi.org/10.1007/s11214-010-9692-5>, doi:10.1007/s11214-010-9692-5.